

# Zinc Oxide Nanowires Grown by Vapor-Phase Transport Using Selected Metal Catalysts: A Comparative Study

Zuoming Zhu,<sup>†</sup> Tsung-Liang Chen,<sup>‡</sup> Yi Gu,<sup>†</sup> John Warren,<sup>§</sup> and Richard M. Osgood, Jr.\*<sup>\*,†,‡,§</sup>

*Department of Applied Physics and Applied Mathematics and Department of Electrical Engineering, Columbia University, New York, New York 10027, and Center for Functional Nanomaterials, Brookhaven National Laboratory, Upton, New York 11973-5000*

*Received March 15, 2005. Revised Manuscript Received May 13, 2005*

We report a comparative study of metal-surface-catalyzed ZnO nanowire growth. The growth is initiated on Si and sapphire substrates, which were prepared with thermal vapor deposited thin metallic films. As described earlier for Au films, these films may change morphology at growth temperatures and catalyze ZnO nanowire growth. Here we use materials diagnostics based on synchrotron X-ray diffraction, transmission electron microscopy, field emission scanning electron microscopy, photoluminescence, and energy-dispersive X-ray spectroscopy to compare the growth from Au, Ag, Fe, and Ni catalysts. We relate the materials properties of the ZnO nanowires to the substrate and catalyst surface structure and comment on the possible growth modes using each of these metal catalysts.

## I. Introduction

Nanowire growth has been investigated as a route to low-dimensional crystal structures.<sup>1–8</sup> These structures are potentially applicable to a variety of optical- and electronic-device applications, such as lasers or light-emitting diodes.<sup>6,9–11</sup> While the growth of these wires has been achieved under a wide variety of conditions, including liquid<sup>5,12,13</sup> and vapor growth,<sup>7,8,14</sup> one of the most reliable and well-studied approaches has used vapor-phase transport of the constituents coupled with surface catalysis of the nucleation and growth steps. Yang and his collaborators have described an excellent example of this approach for the growth of ZnO nanowires.<sup>6,8,15,16</sup> In these studies, small surface-bound droplets of Au were formed on a single-crystal surface, such as Si(100),

through heating of a thin Au film, deposited on the Si surface. These droplets served as alloying sites for condensation of Zn vapor from a nearby solid-ZnO source.<sup>16</sup> Single-crystal ZnO nanowires then grew from the supersaturated AuZn alloy, in the presence of constant trace amounts of oxygen. The orientation of the wires was shown to be governed by registration on the substrate crystalline lattice.<sup>16</sup>

Despite the success of this method, there have been relatively limited comparative studies of such growth using other metal catalysts and on other surfaces. Such studies are useful because both the catalyst and substrate play important roles in the properties and the structure of the nanowires. In addition, attainment of good nanowire material properties, such as good crystallinity and low impurity concentration, play an important role in the practicality of various nanowire applications in electronics and optics.

In this paper, we have undertaken the study of ZnO nanowire growth using four different metal catalysts and using substrates of differing elemental materials, structure, and crystal orientation. We also have employed multiple materials diagnostics to characterize the material, optical, and structural properties of the nanowires grown using these different substrate systems.

## II. Experimental Section

**Nanowire Growth.** Our ZnO nanowire growth is achieved by surface-catalyzed vapor-phase transport. In this method, mixed ZnO and graphite powder (molar ratio 1:1) react under high temperature and generate the Zn vapor carried by argon through a narrow-bore (2-cm diameter, 76.2-cm length) quartz tube mounted in a variable-temperature furnace. A metal catalyst present on the sample substrate, mounted downstream from the Zn source, causes alloying of the catalyst with Zn vapor until Zn supersaturation is reached.

\* Corresponding author. Fax: (212)-860-6182. E-mail: osgood@columbia.edu.

<sup>†</sup> Department of Applied Physics and Applied Mathematics.

<sup>‡</sup> Department of Electrical Engineering.

<sup>§</sup> Brookhaven National Laboratory.

- Hicks, L. D.; Dresselhaus, M. S. *Phys. Rev. B* **1993**, *47*, 16631.
- Alivisatos, A. P. *Science* **1996**, *271*, 933.
- Lieber, C. M. *Solid State Commun.* **1998**, *107*, 607.
- Hu, J. T.; Odom, T. W.; Lieber, C. M. *Acc. Chem. Res.* **1999**, *32*, 435.
- Holmes, J. D.; Johnston, K. P.; Doty, R. C.; Korgel, B. A. *Science* **2000**, *287*, 1471.
- Huang, M. H.; Mao, S.; Feick, H.; Yan, H. Q.; Wu, Y. Y.; Kind, H.; Weber, E.; Russo, R.; Yang, P. D. *Science* **2001**, *292*, 1897.
- Dai, Z. R.; Pan, Z. W.; Wang, Z. L. *Adv. Funct. Mater.* **2003**, *13*, 9.
- Yang, P.; Yan, H.; Mao, S.; Russo, R.; Johnson, J.; Saykally, R.; Morris, N.; Pham, J.; He, R.; Choi, H.-J. *Adv. Funct. Mater.* **2002**, *12*, 323.
- Duan, X. F.; Huang, Y.; Agarwal, R.; Lieber, C. M. *Nature* **2003**, *421*, 241.
- Gudiksen, M. S.; Lathon, L. J.; Wang, J.; Smith, D. C.; Lieber, C. M. *Nature* **2002**, *415*, 617.
- Duan, X. F.; Huang, Y.; Cui, Y.; Wang, J. F.; Lieber, C. M. *Nature* **2001**, *409*, 66.
- Trentler, T. J.; Hickman, K. M.; Goel, S. C.; Viano, A. M.; Gibbons, P. C.; Buhro, W. E. *Science* **1995**, *270*, 1791.
- Peng, X. G.; Manna, L.; Yang, W. D.; Wickham, J.; Scher, E.; Kadavanich, A.; Alivisatos, A. P. *Nature* **2000**, *404*, 59.
- Chen, C. C.; Yeh, C. C. *Adv. Mater.* **2000**, *12*, 738.
- Wu, Y. Y.; Yan, H. Q.; Huang, M.; Messer, B.; Song, J. H.; Yang, P. D. *Chem. Eur. J.* **2002**, *8*, 1261.

- Huang, M. H.; Wu, Y.; Feick, H.; Tran, N.; Weber, E.; Yang, P. *Adv. Mater.* **2001**, *13*, 113.

As pure zinc forms at the surface of the alloyed catalyst, it is then oxidized by the low concentration of oxidizing gas, CO/CO<sub>2</sub>, and seeded crystal growth of ZnO occurs.<sup>16</sup>

In the growth system, the sample and reactant were placed in different temperature regions of the 2-cm-diameter quartz tube. The temperature of the source was kept between 850 and 950 °C, while the sample was kept at a temperature of 800–900 °C; the argon flow was set to be from 30.2 to 40 sccm. Each substrate (sapphire/silicon) was cleaned for 30 min using a supersonic bath of acetone, methanol, and deionized water before deposition of its metallic thin film and then dried in N<sub>2</sub>. No effort was made to remove the ~20-Å-thick native oxide on the silicon surfaces. The thin-film metal catalyst was deposited on the substrates by thermal evaporation.

**Characterization.** The crystal structure of our ZnO nanowires was characterized with synchrotron X-ray diffraction (XRD). The X-ray diffraction measurements were taken at Beamline  $\times 18A$  at the National Synchrotron Light Source (NSLS) of Brookhaven National Laboratory. The incident X-ray beam was focused by a bent, cylindrical, platinum-coated aluminum mirror and “slitted” to dimensions of 0.5 mm, vertical, and 1 mm, horizontal. The wavelength was selected to be 1.2915 Å (corresponding to a photon energy of 9.6 keV) by a double-flat-crystal-Si(111) monochromator. The samples were mounted onto a Huber four-circle diffractometer. An avalanche-photodiode detector was used to collect the scattered beam.

The surface morphologies of those nanowires were examined using scanning electron microscopy (SEM, JEOL 5600L), and detailed observation was done with a field-emission scanning electron microscope (FE-SEM, JEOL 6500-F) at Brookhaven National Laboratory. For the case of Ni-catalyst samples, transmission electron microscopy (TEM; JEM 100CX) was employed to analyze the nanowires profiles. The nanowire samples were scraped from the as-grown layer. The TEM measurements were taken using an accelerating voltage of 100 kV and prepared by depositing a hexane solution of nanowires on a copper-grid backed with Formvar.

The compositional analysis of as-synthesized nanowires was done by energy-dispersive X-ray (EDX) spectrum obtained using an EDAX Phoenix Pro detector, attached to an SEM (LEO 1455 VP), at an electron energy of 15 keV. Periodically the beam position was moved to check for the presence of any beam damage. The spectra typically contained multiple prominent features of the elements of interest, such as the K line of oxygen and K and L lines of Zn. In addition, the presence or absence of catalyst metal could also be examined through features such as the M line of Au.

The optical properties of nanowires were measured by photoluminescence (PL). The PL was recorded with a <sup>3</sup>/<sub>4</sub> m monochromator equipped with a GaAs photomultiplier operating in its photon-counting mode. Samples were excited by the 325-nm emission from a He–Cd laser with a 10 mW maximum power; the incident power intensities were varied from 0.28 to 28 W/cm<sup>2</sup> using a neutral density filter. The spectra were measured from room temperature to 10 K, although only room-temperature data is reported here.

### III. Results and Discussion

In this section, we describe the growth and growth mechanisms of ZnO wires using four different catalytic metals. The section is organized according to the materials properties obtained from the characterization probes used in our investigation, including surface morphology, crystal structure, composition, and optical properties. In the section on surface morphologies, our data is further organized by each of the four catalyst types used here.

**1. Morphologies (SEM and TEM).** *1.1. Noble-Metal Catalysts. Gold.* Au is the best-known noble-metal catalyst for the growth of one-dimensional ZnO nanostructures via vapor-phase transport. As mentioned above, previous studies with Au-island catalyst have shown that ZnO nanowires grow via a vapor–liquid–solid (VLS) mechanism.<sup>15,16</sup> Thus, our initial experiments used a Au thin-film catalyst so as to allow comparison with prior work. Our catalyst was typically 1–10 nm in thickness, deposited via thermal evaporation with the substrate at room temperature. As the Au thin film was being raised to the growth temperature, it melted to form isolated surface Au nanoclusters due to the lack of wetting at the Au/Al<sub>2</sub>O<sub>3</sub> interface. Note that due to their small size, nanoclusters from Au thin films are excellent catalysts for the growth of nanometer-scale ZnO wires. Figure 1a,d display typical SEM images for ZnO nanowires grown on Si(111) and *a*-plane sapphire substrates from an initial 2.5-nm-thick Au film. Growth was performed at  $T_{\text{sub}} \approx 870$ –880 °C for 30 min on Si(111) substrates. The nanowire yield was particularly high, with high spatial uniformity. For 30-min growth at 870 °C, the wires had diameters ranging from 100 to 200 nm and lengths from 1 to 6  $\mu\text{m}$ . A high-magnification field-emission SEM image (see inset of Figure 1a) shows that the nanowires grew “tilted” out of the Si(111) substrate surface. Tilted SEM measurements also showed that on Si(111) substrates these wires grow at angles with respect to the surface normal, which are random with no preferred directions. Finally, these wires had hexagonal cross sections, a shape that is characteristic of the rapid anisotropic growth of ZnO nanowires along the [0001] direction and has been reported in other studies.<sup>17</sup>

The effects of substrate temperature and Au thin-film thickness on the morphologies of nanowires were also investigated. It was found that elevation of the substrate temperature above ~920 °C resulted in crystal overgrowth and deterioration of spatial uniformity (see Figure 1b). In addition, our micrographs showed that the diameters and areal density of the nanowires increased with increasing coverage of the catalyst-metal islands; e.g., ZnO nanorods were observed for the case of thicker, e.g. ~5 nm, Au films on Si(111) (see Figure 1c). In addition, in most cases the presence of Au–Zn alloy on the tips of nanowires was clearly observed in Figure 1c, indicating the presence of the VLS growth mode. Our results also showed that the size of the metal-catalyst droplet increases with increasing catalyst film thickness, thus leading to the growth of thicker nanowires. Our observations are, thus, in general agreement with the dependence of the dimensions of the nanowires on the catalyst-film thickness, which had been reported earlier for the VLS growth of nanowires using metal thin-film catalysts.<sup>8</sup>

Growth was also examined for the case of Au on *a*-plane (110) sapphire, since earlier reports had indicated that growth orientation differed on this substrate.<sup>8</sup> In our case, ZnO nanowires were grown under conditions that yield a range of 60–200 nm in diameter and 5–10  $\mu\text{m}$  in length. Further,

(17) Lyu, S. C.; Zhang, Y.; Ruh, H.; Lee, H.-J.; Shim, H.-W.; Suh, E.-K.; Lee, C. J. *Chem. Phys. Lett.* **2002**, *363*, 134.

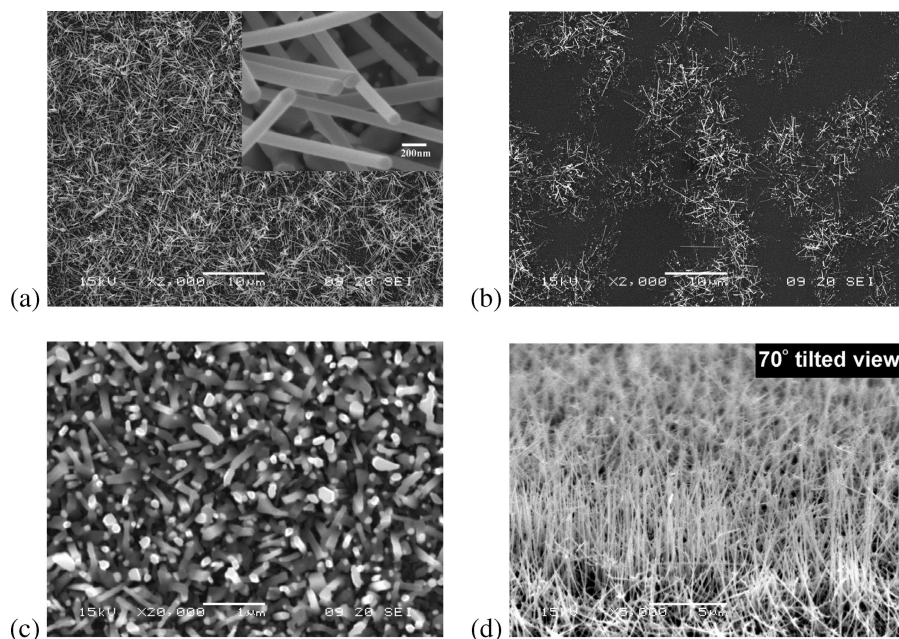


**Figure 1.** Typical SEM images for ZnO nanowires grown on Au-coated (a–c) Si(111) substrates and (d) *a*-plane sapphire substrate. The growth condition are (a) 2.5 nm Au/Si(111) at a substrate temperature of  $T_{\text{sub}} \approx 870$  °C, (b) 2.5 nm Au/Si(111) at  $T_{\text{sub}} \approx 930$  °C, (c) 5 nm Au/Si(111) at  $T_{\text{sub}} \approx 870$  °C, and (d) 2.5 nm Au/*a*-plane sapphire at  $T_{\text{sub}} \approx 870$  °C.

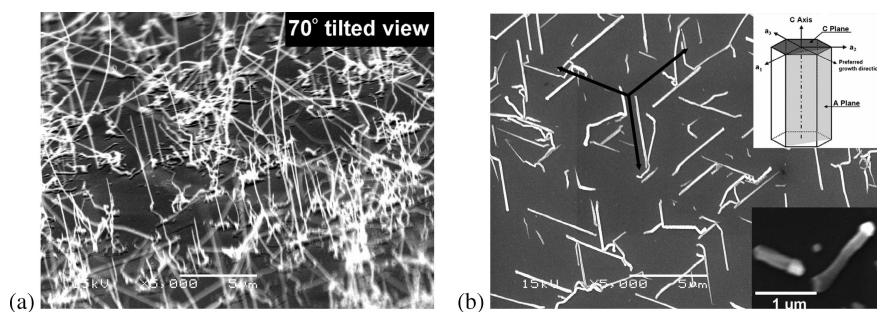


**Figure 2.** SEM images of nanowires grown on (a) *a*-plane (110) and (b) *c*-plane (001) sapphire substrates starting at room temperature with 2.5-nm Ag thin films. Growth occurred at  $T_{\text{sub}} \approx 850$  °C for 30 min. The inset at the upper right corner of Figure 2b shows a descriptive sketch of the hexagonal structure of sapphire and preferred growth direction of the ZnO nanowires. The other inset in the lower right corner of Figure 2b shows that catalyst-alloy nanoclusters at low substrate temperature or growth time were observed on the nanowire tips.

the nanowires grew vertically on *a*-plane sapphire substrate. As previously reported,<sup>6</sup> this growth orientation is a result of good lattice match (mismatch < 0.08%) between the ZnO (001) plane and sapphire (110) plane.

**Silver.** Compared with gold, silver has been much less explored as a catalyst for the growth of ZnO nanowires. Ag has generally similar properties to Au in terms of the formation of nanoclusters from a melted thin silver film. On the other hand, it does have a lower melting point and is more reactive, i.e., it readily oxidizes to form either a Ag<sub>2</sub>O or, at higher oxygen exposure, a AgO surface layer.<sup>18</sup> Despite these differences, Ag thin films have also been used as catalysts for the growth of ZnO wires. For example, in one experiment, Heo et al. reported molecular beam epitaxy growth of ZnO nanorods on Si/SiO<sub>2</sub> substrates using a Ag thin-film catalyst.<sup>19</sup> In the present work, we have investigated the growth of ZnO nanowires on two differently oriented sapphire substrates, i.e., the (110) and (001) planes, using Ag thin-film catalysts. To our knowledge there have been

no previous reports of ZnO nanowire growth using the Ag/Al<sub>2</sub>O<sub>3</sub> system.

Figure 2a,b shows SEM images of nanowires grown on *a*-plane (110) and *c*-plane (001) sapphire substrates starting at room temperature with 2.5 nm Ag thin films. Growth occurred at  $T_{\text{sub}} \approx 850$  °C for 30 min. The wire growth was dense but disordered, i.e., the diameters of the nanowires ranged from 70 to 250 nm and their lengths were 0.5–5 μm. In addition, as shown in Figure 2, the as-grown nanowires are nonuniform, i.e., they display growth kinks. These kinks may be a result of nanowire growth instabilities when using silver catalysts. This nonuniformity and disorder are most probably because the growth temperature needed for nanowire growth is significantly above the relatively low melting point of Ag thin films. As a result of this high growth temperature and long growth times, it was observed that the Ag–Zn alloy tips evaporated prior to the end of growth; see Figure 2. This evaporation caused growth to cease on wires where the catalyst was fully depleted. However, at reduced substrate temperature and growth time, catalyst-alloy nanoclusters were clearly present on the nanowire tips (see the inset of Figure 2b); this observation indicates that the growth of nanowires is due also to the VLS process.

(18) Waterhouse, G. I. N.; Bowmaker, G. A.; Metson, J. B. *Appl. Surf. Sci.* **2001**, *183*, 191.

(19) Heo, Y. W.; Varadarajan, V.; Kaufman, M.; Kim, K.; Norton, D. P.; Ren, F.; Fleming, P. H. *Appl. Phys. Lett.* **2002**, *81*, 3046.

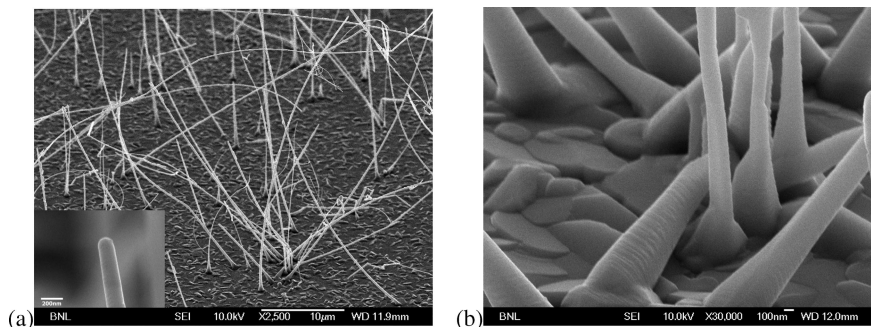


**Figure 3.** (a) A 60°-tilted FE-SEM image of ZnO nanowires grown on *a*-plane (110) sapphire substrate prepared with a 2.5-nm Fe thin film. Growth was at  $T_{\text{sub}} \approx 890\text{--}900\text{ }^{\circ}\text{C}$  for 30 min. The inset displays a typical high-magnification FE-SEM image taken at the tip of an Fe-catalyzed nanowire; no alloy nanoclusters are seen at the tip. (b) A high-magnification FE-SEM image of the base of the nanowires shown in Figure 3a.

Our results with Ag show that the growth direction of the nanowires again depends strongly on substrate orientation; thus, the results are similar to that seen with Au thin-film catalysts. The inset of Figure 2b shows a descriptive sketch of the hexagonal structure of sapphire and preferred growth direction of ZnO nanowires. Figure 2a also shows that ZnO nanowires grew nearly vertically on *a*-plane (110) sapphire, as was also seen in the case of Au catalyst. In particular, ZnO has a wurzite structure, with lattice constants  $a = 3.24\text{ \AA}$  and  $c = 5.19\text{ \AA}$ . The growth of ZnO nanowires is generally along the  $\langle 001 \rangle$  direction. A previous study by Huang et al., using Au catalysts, showed that because the ZnO *a*-axis and sapphire *c*-axis are related almost by a factor of 4, i.e., this mismatch was  $< 0.08\%$  at room temperature, ZnO nanowires grow epitaxially and vertically on the (110) plane of sapphire.<sup>16</sup>

Interestingly, oriented growth was also obtained for Ag on *c*-plane (001) sapphire. As shown in Figure 2b, the nanowires grew on the  $\text{Al}_2\text{O}_3$  surface along the directions of the three 2-fold  $\langle 110 \rangle$  axes of sapphire. Note that for a focused SEM image as shown in Figure 2b, there are no appreciable differences in image sharpness for either of the two ends of the wires, thus suggesting that most wires fully lie in plane of the surface. A similar result has also been seen for the case of Si nanowires.<sup>15</sup> In this case, Si nanowire arrays grow vertically on Si(111) substrate; however, when a Si(100) substrate is used, three sets of oriented Si nanowire arrays grow out of the substrate surface along the three equivalent  $\langle 111 \rangle$  directions.

**1.2. Transition-Metal Catalysts.** In contrast to the use of noble metals, transition metals (TM) have not been yet reported as catalysts for ZnO nanowire growth by vapor-phase transport. However, transition-metal oxides, such as nickel oxides, have recently been found to be effective catalysts for semiconductor nanowire growth using either VLS or vapor–solid (VS) processes.<sup>17</sup> In this section, we investigate the use of transition-metal films (Fe and Ni) as catalysts for growth of ZnO nanowires by vapor-phase transport. Note that in both cases, these metal films, which were prepared ex-situ, have native surface-oxide layers. The thickness of these layers undoubtedly increases in thickness in the growth furnace.

**Iron.** The transition metal iron has a higher melting point than either Au or Ag. This metal has been extensively used in the catalytic growth of other one-dimensional system, such as carbon nanotubes;<sup>20,21</sup> however, it has not been used

previously in the growth of ZnO nanowires. Because the growth temperature we used here ( $\sim 900\text{ }^{\circ}\text{C}$ ) is much lower than the melting points of Fe ( $1536\text{ }^{\circ}\text{C}$ ), it is unlikely that thin-film melting and metallic-nanocluster formation would occur upon annealing of our Fe thin films. In fact, as seen below, the VLS mechanism apparently does not occur for Fe, and thus the nanowire growth mode is different for the Fe than for the noble-metal (Au or Ag) thin-film catalysts.

Figure 3a shows the general morphology of ZnO nanowires grown on *a*-plane (110) sapphire substrate prepared with a 2.5-nm Fe thin film. Growth was at  $T_{\text{sub}} \approx 890\text{--}900\text{ }^{\circ}\text{C}$  for 30 min. Note that the growth parameters were nearly the same as for the case of the noble metals. The 60°-tilted FE-SEM image in Figure 3a shows that the diameter of the base and tip of the nanowires are  $\sim 550$  and  $90\text{ nm}$ , respectively; their lengths were  $\sim 10\text{--}50\text{ }\mu\text{m}$ . The areal density of nanowires is  $\sim 0.05/\mu\text{m}^2$ , which is much lower than that observed for the case of the noble metal thin-film catalysts. This low areal density may originate from the differences in growth mechanisms for the noble-metal catalysts; see the discussion below.

There are two possible mechanisms for the growth of one-dimensional ZnO nanostructures using vapor-phase transport, namely VLS<sup>16,22</sup> and VS processes.<sup>23,24</sup> As mentioned above, ZnO nanowires clearly grow through the VLS mechanism in the case of Au and Ag catalysts. To briefly review the VLS process, the growth of this nanostructure is guided by the initial formation of a liquid-alloy droplet. This melt-formed nanodroplet absorbs the incoming vapor reactant Zn and then forms a liquid-alloy droplet. As the concentration of Zn in the liquid droplet reaches supersaturation, a one-dimensional nanostructure grows by means of Zn precipitation at the interface between droplet and substrate followed by oxidation of the Zn. One prime indicator of the VLS growth process is the presence of an alloy nanocluster at the tip of one-dimensional nanostructures;<sup>15,16</sup> this is seen, for example, in the case of Au and Ag. On the other hand, in the VS mechanism, oxide vapor, evaporated from the source material in a high-temperature region (in most cases, pure oxide powder is directly employed as a source material),

- (20) Cassell, A. M.; Raymakers, J. A.; Kong, J.; Dai, H. J. *J. Phys. Chem. B* **1999**, *103*, 6484.  
 (21) Hernadi, K.; Fonseca, A.; Nagy, J. B.; Bernaerts, D.; Lucas, A. A. *Carbon* **1996**, *34*, 1249.  
 (22) Wagner, R. S.; Ellis, W. C. *Appl. Phys. Lett.* **1964**, *4*, 89.  
 (23) Pan, Z. W.; Dai, Z. R.; Wang, Z. L. *Science* **2001**, *291*, 1947.  
 (24) Yang, P. D.; Lieber, C. M. *J. Mater. Res.* **1997**, *12*, 2981.

is transported and directly deposited onto a substrate in a lower temperature region. Substrate surface defects or dislocations then provide energetically favorable nucleation sites for the incoming oxide vapor, on which wirelike nanostructures grow through the continuous condensation and deposition of oxide vapor. Thus, various wirelike nanostructures, such as nanobelts,<sup>7,23</sup> nanorods,<sup>24</sup> and nanowires<sup>25</sup> have been grown via the VS process. It has also been suggested that in the VS mechanism the formation of wirelike nanostructures might be controlled by kinetics during crystal growth.<sup>7,25</sup> In general, the growth temperature and the supersaturation ratio are two dominant factors in controlling the morphology of the wirelike structures;<sup>7</sup> while the growth temperature and supersaturation ratio as well as the nucleation-site size are critical factors for defining the cross sectional width or diameter of the wirelike nanostructures.<sup>7,24</sup> More detailed discussions on anisotropic growth kinetics in the VS mechanism can be found in refs 7 and 26.

The inset of Figure 3a shows a typical high-magnification FE-SEM image taken at the tip of an Fe-catalyzed nanowire in Figure 3a; no alloy nanocluster is seen at the tip. Attempts to observe alloy nanoclusters on the nanowire tips after lowering the substrate temperatures or reducing the growth time were also not successful. Alternatively, reducing growth time yielded shorter wires but still yielded no observation of alloy nanoclusters. In addition, since a catalyst droplet drives VLS growth of nanowire, the diameter of the nanowire usually varies with the initial catalyst film thickness (see above). However, in the case of Fe, the diameter of the nanowires was insensitive to the Fe thin-film thickness. Our results suggest that in the case of Fe, nanowires do not grow via the VLS process.

Figure 3b shows a high-magnification FE-SEM image of the base of the nanowires in Figure 3a. Note that the surface appears to be covered by a thin buffer layer formed prior to the nanowire growth, most probably some form of ZnFe mixed oxide (see below), and that the nanowires thus do not grow directly on the sapphire substrate but appear to originate from "cracks" in the ZnO thin buffer layer on the sapphire substrate. Since growth does not occur on a clean sapphire surface, the Fe thin film plays a key role in the formation of the buffer layer and the subsequent growth of nanowires. To see any effects of Fe film morphology, a 2.5-nm Fe-covered sapphire substrate was annealed at  $\sim 900$  °C for 5 min, without any ZnO growth. It was found that this thermal treatment produced about 500-nm to 1- $\mu$ m-diameter islands on the substrate; these islands were similar in geometry to the cracking pattern of the ZnO buffer layer observed in Figure 3b. This cracking is most probably due to the mismatch in thermal expansion in the Fe/sapphire materials system, which has coefficients of thermal expansion of 12.6 and  $7.5 \times 10^{-6} \text{ K}^{-1}$  for Fe and  $\text{Al}_2\text{O}_3$ , respectively.<sup>27</sup> Note also that the melting point of Fe (1538 °C) is much higher than the  $\sim 900$  °C growth temperature used here.

On the basis of these observations, we propose that for the Fe thin-film catalysts, the growth of ZnO nanowires may occur via a VS process.<sup>23,24</sup> We suggest that the process

proceeds as follows: First, Zn vapor is generated by thermal carbon reduction of the ZnO powder and transported to substrate surface, where the incoming Zn vapor is preferentially adsorbed on the large Fe islands formed at the 900 °C growth temperature. With the increase of the Zn concentration, instead of precipitating zinc, zincite-phase buffer layers are formed on the substrate in the form of either Fe–Zn–O alloy or zinc oxide. A study of the phase diagram of the Fe–O–Zn system by Degterov et al. shows that at 900 °C the alloy of Fe–Zn–O remains zincite phase when the molar composition of Fe is below about 20%.<sup>28</sup> Subsequently, the rough nature of the large islands on the fissured ZnO buffer layers serves as energetically preferred absorption sites for the incoming vapor Zn, for condensation and nucleation. As the Zn vapor continues to be deposited onto these nucleation sites, it is immediately oxidized, and nanowires are formed through a VS process. Note that due to the good epitaxial lattice match (mismatch < 0.08%) between the ZnO (001) plane and sapphire (110) plane, the ZnO buffer layer most probably grows along the [0001] direction; subsequently, the nanowires grow epitaxially along the [0001] direction. This good epitaxial lattice match is consistent with our experimental observations of most nanowire types, which grow perpendicularly (e.g., see above for the case of Au). Finally, it is worth pointing out here that a major difference in the relative chemical reactivity of iron and the noble-metal catalysts may result in the difference in nanowire growth mode for iron catalyst and noble-metal catalysts. In particular, iron metal is more reactive with oxygen than zinc; as a result, it is unlikely to form a stable Fe/Zn alloy under the oxidizing atmosphere required to initiate VLS growth. Instead, a stable nonreactive Fe/Zn oxide is formed on the substrate first and subsequently the wires grow via a VS process. However, when the noble metals, i.e., gold and silver, are employed as catalysts, a zinc–noble metal alloy is formed first. The steady dissolution of zinc, followed by its oxidation, will prevent the oxidation of these metal or metal alloys, allowing the wire to grow via a VLS mechanism.

*Nickel.* The growth of ZnO nanowires using Ni catalyst was investigated because of recent reports of using nickel oxides as catalysts for the growth of ZnO wires.<sup>17</sup> Figure 4a presents a 60°-tilted FE-SEM image of ZnO nanowires grown on *a*-plane sapphire with 2.5-nm Ni thin film overlayer. Growth was at  $T_{\text{sub}} \approx 890\text{--}900$  °C for 30 min. The synthesized ZnO nanowires were typically about 60–180 nm in diameter and 4–20  $\mu\text{m}$  in length. The aspect ratio of the wires is thus  $\sim 50\text{--}200$ . Although in this figure the nanowires are generally tilted away from the substrate normal, the overall growth direction is approximately vertical. In addition, note the presence of spherical ZnO nanoparticles on the substrate between the nanowires. These ZnO nanowires were also examined using transmission electron microscopy. Figure 4b displays a TEM image of a segment of a single nanowire and its selected-area electron diffraction

(25) Yin, Y. D.; Zhang, G. T.; Xia, Y. N. *Adv. Funct. Mater.* **2002**, *12*, 293.

(26) Blakely, J. M.; Jackson, K. A. *J. Chem. Phys.* **1962**, *37*, 428.

(27) Vispute, R. D.; Talyansky, V.; Choopun, S.; Sharma, R. P.; Venkatesan, T.; He, M.; Tang, X.; Halpern, J. B.; Spencer, M. G.; Li, Y. X.; Salamanca-Riba, L. G.; Iliadis, A. A.; Jones, K. A. *Appl. Phys. Lett.* **1998**, *73*, 348.

(28) Degterov, S. A.; Jak, E.; Hayes, P. C.; Pelton, A. D. *Metall. Mater. Trans. B–Proc. Metall. Mater. Proc. Sci.* **2001**, *32*, 643.

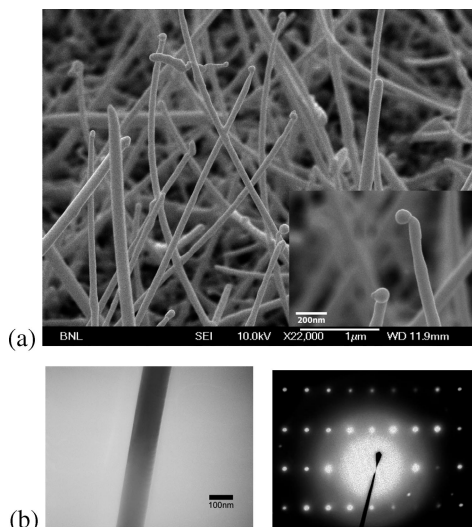


**Figure 4.** (a) A 60°-tilted FE-SEM image of ZnO nanowires grown on *a*-plane sapphire with 2.5-nm Ni thin film overlayer. Growth was at  $T_{\text{sub}} \approx 890\text{--}900\text{ }^{\circ}\text{C}$  for 30 min. The inset shows solidified spherical nanoclusters on the tips of some ZnO nanowires. (b) A TEM image of a segment of a single nanowire and a selected-area electron diffraction pattern taken from it.

(SAED) pattern. The image indicates that the wires are single-crystal with growth along the [0001] direction.

Ni has a somewhat lower melting point than Fe, i.e., 1453 °C vs 1538 °C. Thus it would be reasonable to expect the same nanowire growth mode when using Ni as catalyst rather than Fe. However, our observations suggest that the actual growth appears to show evidence of being a combination of the two mechanisms seen above for Fe and the noble metals. In particular, for the FE-SEM measurements of wires grown by Ni thin-film catalysts on sapphire substrates, there was no visual evidence of thermally formed cracks on substrates, as was typically seen in the case of Fe. On the other hand, as shown in the inset of Figure 4a, solidified spherical nanoclusters were observed on the tips of some ZnO nanowires. These results indicate that, as in the case of Au and Ag, the growth of ZnO nanowires from the Ni catalyst is apparently dominated by vapor–liquid–solid growth. One possibility, which has been seen in the case of carbon CVD on Ni/sapphire catalysts,<sup>29</sup> is that the Ni thin film may form Ni–Zn alloy islands through absorption of incoming Zn vapor. However, our experimental evidence is relatively sparse and thus we cannot unequivocally rule out the occurrence of the VS mode in the case of Ni. More direct experimental evidence such as HRTEM measurement on the nanoclusters' tip region of the wires is needed.

**2. Crystal Structure (XRD).** Synchrotron X-ray diffraction was used to determine the crystal structure of the as-synthesized ZnO nanowires. Figure 5a shows a comparison of the XRD patterns for ZnO nanowires grown on a Au/Si(111) substrate with high-purity ZnO powder (Alfa Aesar). The XRD pattern of the nanowires shows a high degree of crystallinity; the diffraction peaks can be indexed to the hexagonal wurtzite structure of bulk ZnO with lattice constants of  $a = 3.252\text{ \AA}$  and  $c = 5.213\text{ \AA}$ . In addition to diffraction peaks from the Au catalyst, no other peaks due

to impurity phases were observed. Note that as seen in Figure 5a, the XRD peaks for nanowires were broader than that of the bulk ZnO powder. While our wires have cross sections much smaller than the characteristic diameter of the powder, i.e.,  $\sim 0.2\text{ }\mu\text{m}$  versus  $1\text{ }\mu\text{m}$ , respectively, the wires are still large enough to not show X-ray diffraction finite-size broadening of the magnitude shown in Figure 5. Instead, we tentatively attribute the broadening to a distribution of strain in the wire samples due to different degrees of bending, etc (see Figures 1d and 3a, for example); however, more experimentation is necessary to confirm this explanation.

XRD measurements were also made on the ZnO nanowires synthesized using other metal catalysts. As for the case of growth using Au/Si(111), for all catalysts, the XRD diffraction peaks could be indexed to be those of hexagonal wurtzite ZnO. In addition, it was found that the relative intensities of the major characteristic XRD diffraction peaks were closely related to the degree of nanowire lattice alignment on the growth substrates. In particular, Figure 5b shows a series of XRD patterns, which were recorded at angles covering three major characteristic XRD diffraction peaks of the nanowires of wurtzite ZnO. For the case of Au/Si(111), for which the nanowires grew randomly “tilted” out of the substrate surface, the relative intensities of the XRD diffraction peaks of nanowires are similar to those obtained by standard ZnO powder diffraction. In the case of Fe and Au catalysts on *a*-plane sapphire, the diffraction pattern of the nanowires shows a much higher (002) peak intensity compared with that observed in ZnO powder diffraction, which has its maximum intensity for the (101) peak. This change in intensity pattern for the nanowires is consistent with the nanowires growing nearly vertically on the substrate and along the *c*-axis in the cases of the Fe and Au catalysts. In fact, if the nanowires were perfectly vertically aligned on substrates and grew perfectly along the *c*-axis, only the diffraction peaks from the (00*l*) plane could be observed in the XRD pattern.<sup>8</sup> In the case of the Ni catalyst on *a*-plane sapphire, the relative intensity of the (002) peak is lower than that for Fe and Au because the growth direction is only approximately vertical. Note also that, in the case of Fe, the XRD diffraction peaks come not only from the nanowires but also from the buffer layers observed in Figure 3b. In addition, in the case of the Fe catalyst no signals from metallic Fe or its oxides are detected in the full XRD pattern; this result is consistent with our suggestion that the Fe thin film alloys with Zn and O to form zincite-phase buffer layers.

**3. Composition Analysis (EDX).** The chemical composition of as-synthesized nanowires was analyzed by EDX. Figure 6 shows a series of EDX patterns of the nanowires synthesized using several different metals. To make a meaningful comparison, the growth time, source temperature, and flow rate for each sample were chosen to be the same; however, due to the varying growth properties, the growth temperature was chosen to be typical of the operational range for each catalyst. The results show that nanowires are pure ZnO and have no alloys with any of the catalytic metals within the detection limits of the EDX measurements of approximately  $\sim 1\%$ . Note that the presence of the Al and C signals would be expected due to the sapphire substrate and

(29) Yudasaka, M.; Kikuchi, R.; Ohki, Y.; Yoshimura, S. *J. Vac. Sci. Technol. A* **1998**, *16*, 2463.

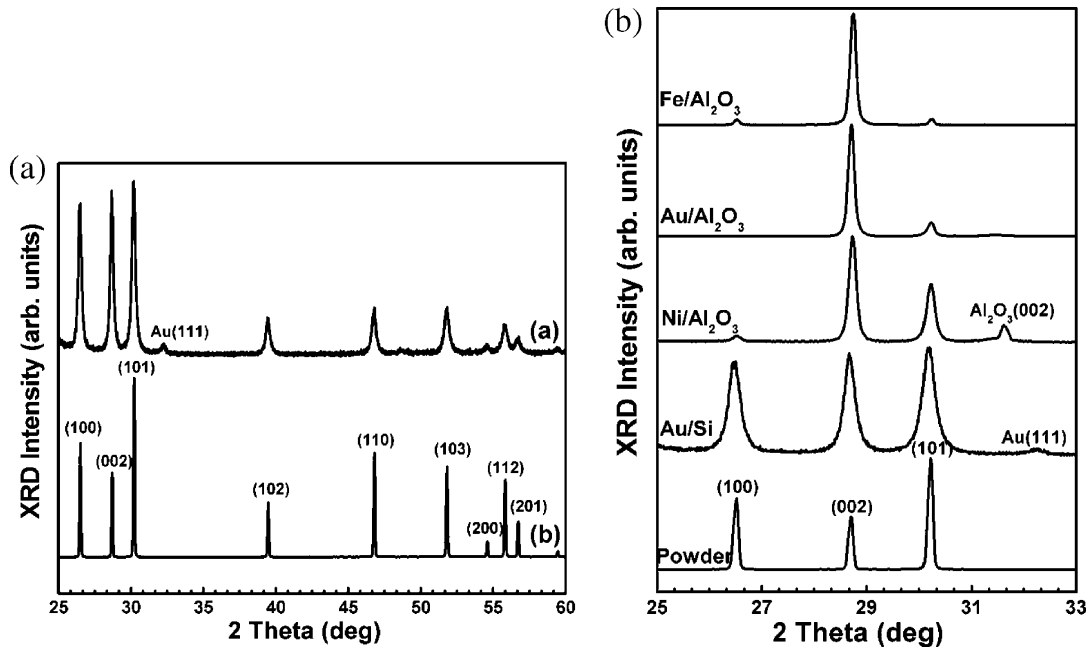


**Figure 5.** (a) A comparison of the XRD patterns for ZnO nanowires grown on a Au/Si(111) substrate and high-purity ZnO powder (Alfa Aesar). (b) A series of XRD spectra for ZnO nanowires synthesized using several different metal catalysts. The spectra were recorded at angles covering three major characteristic XRD diffraction peaks of the wurtzite ZnO.

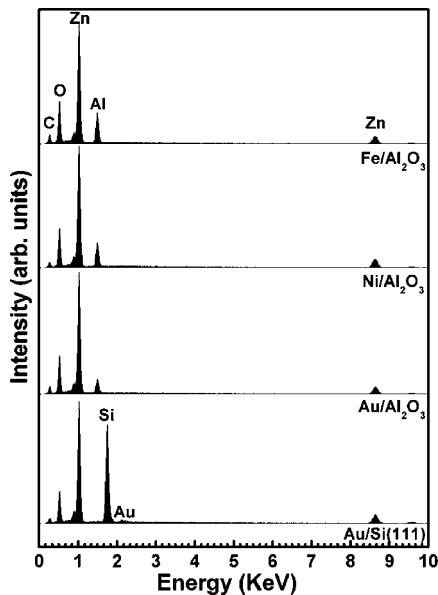


**Figure 6.** A series of EDX patterns of the ZnO nanowires synthesized using several different metal catalysts.

from the carbon film deposited on the samples prior to EDX measurements, respectively.

To obtain the exact nanowire Zn/O atomic ratio, the contribution to the oxygen signal from the substrates, e.g. Al<sub>2</sub>O<sub>3</sub>, which was obtained from the EDX measurement of a bare sapphire substrate, was subtracted from the nanowire signals. Although the absolute values of the O/Zn atomic ratio determined using this method might have systematic errors, the relative values should be more accurate.

These measurements showed that the atomic composition ratio of Zn/O was different for different catalysts, e.g., the atomic ratios of O/Zn, for the case of Au/Si(111) as well as Au, Ni, and Fe on *a*-plane sapphire, were calculated to be 1.25, 1.09, 0.84 and 0.81, respectively. For the case of Au/Si(111), this value may be an overestimate, since the EDX

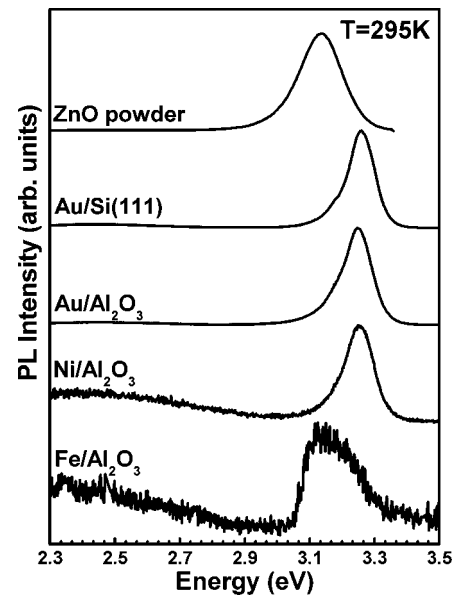


**Figure 7.** Room-temperature PL spectra taken from ZnO nanowires prepared using our three choices of metal catalysts. For comparison, the PL spectrum of high-purity ZnO powder is also included. The intensities have been normalized according to the respective strongest peak.

spectrum will also include a contribution to the O signal due to the oxidized Si substrate. Our results show that the typical O/Zn atomic ratios in the nanowires grown using Fe and Ni catalysts are lower than those for Au catalysts, which indicates that more oxygen vacancies exist in the nanowires grown using Ni and Fe as catalysts. These results are in agreement with the photoluminescence measurements, which are presented in the following section.

**4. Optical Properties (PL).** Measurements of the optical properties of as-grown ZnO nanowires were carried out by PL. Figure 7 shows PL spectra taken from ZnO nanowires prepared using three different choices of metal catalysts. For comparison, the PL spectrum of ZnO powder is also included. Note that all the PL data reported here were done

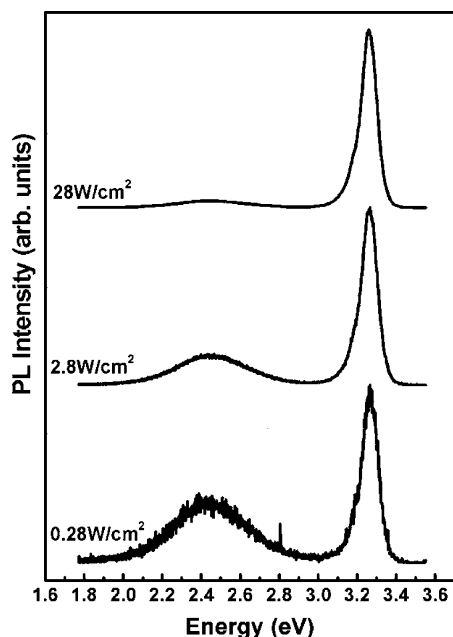


**Figure 8.** PL spectra for ZnO nanowires synthesized using Au-catalyzed growth and measured by different excitation power densities at room temperature. The intensities have been normalized according to the strongest peak.

at room temperature. The detailed temperature dependence of PL spectra of these wires was also investigated; however, these studies will be reported elsewhere. The PL spectrum from ZnO powder was dominated by neutral-donor bound-exciton emission at 3.21 eV with a full width at half-maximum (fwhm) of  $\sim 158$  meV. For all nanowires, except those grown using Fe thin films, a strong ultraviolet peak was observed at 3.26 eV with a narrow fwhm of  $\sim 95$  meV. This feature was attributed to the neutral-donor bound exciton emission.<sup>30</sup> The blue shift and sharpening of exciton emission in nanowire in comparison to results from ZnO powder indicated a higher quality crystal in the nanowires. A very weak green-yellow emission was also observed in the PL spectra of the as-synthesized nanowires. This feature is attributed to emission from the singly ionized oxygen vacancy, in which the photogenerated holes recombine with the electrons.<sup>31</sup> In addition, as can be seen in Figure 7, the intensity of this green/yellow emission relative to that of excitonic emission is stronger in the case of Fe and Ni catalysts than that for the case of Au catalysts. This result is consistent with the EDX data obtained in the last section, which shows that the O/Zn ratios for the former are lower than for the latter.

Finally, the dependence of the PL spectra of nanowires on excitation intensity was examined. Figure 8 shows the PL spectra for ZnO nanowires synthesized using Au-catalyzed growth and measured as a function of excitation intensity. Figure 8 shows that, with increasing power density, the excitonic output emission increases rapidly with respect to the green/yellow emission. This behavior has been

observed before<sup>17,32</sup> and may be due to the fact the density of bound excitonic states is higher than that for the oxygen-vacancy state.

#### IV. Conclusion

In conclusion, this paper reports a detailed, comparative study of metal-surface-catalyzed growth of ZnO nanowires using four different metal catalysts and using substrates of differing materials and crystal orientation. We have employed multiple materials diagnostics to compare the material, structural, and optical properties of the nanowires grown using these different surface systems. In particular, we have found that the growth modes of nanowires are dependent on the choice of surface catalysts, e.g. for the Fe thin-film catalysts, the growth of ZnO nanowires may occur via a vapor–solid process, while, for the case of Au, Ag, and Ni catalysts, the vapor–liquid–solid process usually dominates the wire growth. Further, our study shows that these differences in growth modes are also closely related to the differences in materials properties of these wires, including the degree of nanowire alignment on substrates and the atomic composition ratio of Zn/O, as well as the relative intensity of the oxygen vacancy-related emission in PL spectra.

From a more general point of view, our investigation shows that use of different catalysts provides the versatility of growth for one-dimensional ZnO nanostructures with different ranges of parameters such as diameters, areal densities, and aspect ratios. In particular, our studies suggested that, compared to noble-metal catalysts, growth using transition-metal catalysts occurs at a relatively faster rate and therefore typically yields thicker wires with higher aspect ratio. However, this high growth rate is achieved at the cost of inducing more oxygen vacancies. These differences in growth properties would be expected to affect other properties of wires, such as electrical transports and surface chemistries. Exploration of these aspects will be of interest for practical applications of ZnO wires in nanodevices and chemical sensors.

**Acknowledgment.** The authors thank Steven Ehrlich, Dee Breger, and Abneesh Srivastava for their help with various experimental measurements, Prof. Gertrude Neumark for useful discussions, and an unknown reviewer for the suggestion regarding the nanowire growth mode for the iron catalyst. They gratefully acknowledge the support of this work by the NSF through a grant (Contract No. 0076461) and instrumentation support by the Department of Energy through a grant (Contract No. DE-FG02-90ER14104). The HRSEM and the X-ray diffraction measurements were carried out at the Center for Functional Nanomaterials, Brookhaven National Laboratory, which is supported by the U.S. Department of Energy, Division of Materials Sciences and Division of Chemical Sciences, under Contract No. DE-AC02-98CH10886.

CM050584+

(30) Park, W. I.; Jun, Y. H.; Jung, S. W.; Yi, G.-C. *Appl. Phys. Lett.* **2003**, *82*, 964.

(31) Vanheusden, K.; Warren, W. L.; Seager, C. H.; Tallant, D. R.; Voigt, J. A.; Gnade, B. E. *J. Appl. Phys.* **1996**, *79*, 7983.

(32) Zhu, Z. M.; Li, G. H.; Liu, N. Z.; Wang, S. Z.; Han, H. X.; Wang, Z. P. *J. Appl. Phys.* **1999**, *85*, 1775.